

On the crystal chemistry of sulfur-rich lazurite, ideally $\text{Na}_7\text{Ca}(\text{Al}_6\text{Si}_6\text{O}_{24})(\text{SO}_4)(\text{S}_3)^-\cdot n\text{H}_2\text{O}$

ANATOLY N. SAPOZHNIKOV¹, VLADIMIR L. TAUSON¹, SERGEY V. LIPKO^{1,*}, ROMAN YU. SHENDRIK¹, VALERY I. LEVITSKII¹, LYUDMILA F. SUVOROVA¹, NIKITA V. CHUKANOV², AND MARINA F. VIGASINA³

¹Vinogradov Institute of Geochemistry, Siberian Branch of Russian Academy of Sciences, 1a Favorskii St., Irkutsk, 664033, Russia

²Institute of Problems of Chemical Physics, Russian Academy of Sciences, Chernogolovka, Moscow region, 142432, Russia

³Faculty of Geology, Moscow State University, Vorobievsky Gory, 119991 Moscow, Russia

ABSTRACT

Dark blue lazurite from the Malo-Bystrinskoe lazurite deposit, Baikal Lake area, Eastern Siberian region, Russia, was analyzed by electron microprobe and revealed an unusually high content of total sulfur corresponding to 8.3 wt% S. The relative content of sulfur in sulfate and sulfur in sulfide form was determined by wet chemical analysis. The H₂O content was measured by means of differential thermal analysis in combination with mass spectrometry and infrared (IR) spectroscopy. The charge-balanced empirical formula of lazurite calculated on the basis of 12 (Al+Si) atoms per formula unit was $(\text{Na}_{6.97}\text{Ca}_{0.88}\text{K}_{0.10})_{\Sigma 7.96}[(\text{Al}_{5.96}\text{Si}_{6.04})_{\Sigma 12}\text{O}_{24}](\text{SO}_4)_{1.09}(\text{S}_3)_{0.55}\text{S}_{0.05}\text{Cl}_{0.04}\cdot 0.72\text{H}_2\text{O}$. The presence of H₂O molecules and (S₃)⁻ and (SO₄)²⁻ groups was confirmed by the combination of IR, Raman, electron paramagnetic resonance (EPR), and X-ray photoelectron spectroscopy (XPS) methods. The idealized formula of lazurite is $\text{Na}_7\text{Ca}[\text{Al}_6\text{Si}_6\text{O}_{24}](\text{SO}_4)^2(\text{S}_3)^-\cdot\text{H}_2\text{O}$, and it is believed that extra-framework cations and anions are grouped into clusters of $[\text{Na}_3\text{Ca}\cdot\text{SO}_4]^{3+}$ and $[\text{Na}_4(\text{S}_3)]^{3+}$. The types of isomorphous substitutions in nosean and hauyne are discussed. Lazurite is a clathrate-type mineral, which may be an effective (S₃)⁻ sensor due to the stability of the trisulfur radical anion in isolated cages of the crystal structure. This specific feature makes it possible to study the behavior of this ubiquitous radical anion over larger *T* and *P* ranges as compared to free species. This kind of lazurite, with oxidized and reduced sulfur species, seems to be appropriate for the estimation of the fugacity of SO₂ and O₂ in metasomatic systems forming lazurite-containing rocks. The systematic presence of incommensurate modulations is a unique structural feature of Baikal lazurite and may be an important marker indicating provenance of the mineral.

Keywords: Microporous mineral structure, lazurite, sulfide radical ion, X-ray diffraction, spectroscopy, superstructure

INTRODUCTION

The mineral lazurite belongs to the large family of feldspathoids (so-called cancrinite-sodalite family) whose frameworks contain six-membered rings of Si- and Al-centered tetrahedra. These rings form different strata denoted by the letters *A*, *B*, and *C*. Every ring is linked to three rings of the preceding layer and to three rings of the succeeding layer. The stacking sequence of the *A*, *B*, *C* layers determines the topological type of framework. Minerals and synthetic materials with sodalite-type framework topology (the *ABC*_∞ stacking sequence) are characterized by specific microporous structures with so-called sodalite cages (β-cages) hosting different cations, anions, and neutral molecules. In the current International Mineralogical Association (IMA) list of minerals, the idealized formula of lazurite is given as $\text{Na}_3\text{Ca}(\text{Si}_3\text{Al}_3)\text{O}_{12}\text{S}$.

Lazurite is one of the main components of the rock lapis lazuli, which has long attracted attention as a beautiful ornamental gemstone. Well known are ancient lazurite artifacts, such as vases, boxes, statues, amulets, and carved art products. The State Hermitage Museum (St. Petersburg, Russia) exhibits lazurite-lined countertops and a vase carved from a monolithic

stone. In addition to using the material for stone-cutting products and jewelry, lazurite powder was used in painting. Renaissance artists produced ultramarine, an excellent blue paint prepared from the powder of the “heavenly stone,” wax, and oil. The paint did not fade in the sun and was not damaged by dampness or fire. Ultramarine was used to paint the blue sky, the blue sea, and even the robe of the Virgin Mary. It was applied by Raphael, Leonardo da Vinci, Michelangelo, and many other painters. The paint was considered indispensable, not only for painting but also in dyeing expensive clothes (Ivanov and Sapozhnikov 1985; Gadiyatov 2012).

It was supposed that the blue color of the stone is associated with molecular radical ions (S₃)⁻ and (SO₄)⁻ within its structure (Samoilovich 1971). Most researchers have accepted the relationship between the blue color of lazurite and the radical ion (S₃)⁻ as an indisputable fact (Platonov et al. 1971). Nevertheless, it has been noted that sulfur is present mainly in the form of sulfate in both synthesized and natural S-bearing blue sodalite-type compounds, with the polysulfides concentrated below the detection limit of X-ray absorption near-edge spectroscopy (XANES) and XPS methods (Fleet et al. 2005). According to the EPR data, the color centers observed in lazurite and ultramarine have a “hole” nature, in other words, they form by the loss of an

* E-mail: slipko@yandex.ru

TABLE 1. Formulas of minerals of the sodalite group, the cluster occupancy of the sodalite cages, and values of the unit-cell parameter (*a*)

Mineral	Formula	Occupation (%)	<i>a</i> (Å)	Reference
Sodalite	Na ₈ [Al ₆ Si ₆ O ₂₄]Cl ₂	100[Na ₃ ·Cl] ³⁺	8.882(1)	Hassan and Grundy (1984)
Nosean	Na ₆ [Al ₆ Si ₆ O ₂₄](SO ₄)·H ₂ O	50[Na ₄ ·SO ₄] ²⁺ 50[Na ₄ ·H ₂ O] ⁴⁺	9.084(2)	Hassan and Grundy (1989)
Haüyne	Na _{4.5} Ca ₂ K[Al ₆ Si ₆ O ₂₄](SO ₄) _{1.5} (OH) _{0.5}	75[Na ₃ Ca·SO ₄] ³⁺ 25[K ₂ Ca·OH] ³⁺	9.116(1)	Hassan and Grundy (1991)
Lazurite	Na ₆ Ca ₂ [Al ₆ Si ₆ O ₂₄](SO ₄) _{1.4} S _{0.6}	71[Na ₃ Ca·SO ₄] ³⁺ 29[Na ₃ Ca·S] ^{3+†}	9.105(2)	Hassan et al. (1985)

Note: Mineral structures are determined within the space group $P\bar{4}3n$. However, it is accepted that real sulfate-containing mineral structures consist of two types of domains either of which has ordered structure and symmetry of $P23$ reduced against the space group $P\bar{4}3n$ (Hassan and Grundy 1989).

electron (Samoilovich 1971; Ostroumov et al. 2002).

Lazurite is one of the three cubic sulfate-containing minerals of the sodalite group, and according to the accepted idealized formula of lazurite given in the IMA list of minerals, lazurite is a sodalite-type aluminosilicate with sulfide sulfur prevailing among extra-framework anions. The structure of sodalite-type aluminosilicate minerals is based on the framework [Al₆Si₆O₂₄]⁶⁻, in large cavities of which occur cations Na⁺, Ca²⁺, and K⁺ that compensate the charge of the framework, and additional anions Cl⁻, (SO₄)²⁻, S²⁻, and (OH)⁻. Extra-framework cations and anions form clusters, the composition, size, and charge of which determine the originality of the structure of each particular mineral (Hassan and Grundy 1984, 1989, 1991; see Table 1).

It should be added that the optically anisotropic orthorhombic lazurite Na_{6.4}Ca_{1.5}[Si₆Al₆]₁₂O₂₄(SO₄)_{1.6}(S₃)_{0.2}·0.62H₂O, space group *Pnaa*, *a* = 9.066(2), *b* = 12.851(2), *c* = 38.558(4), *Z* = 6, is approved by IMA (No. 2010-070) as the mineral vladimirivanovite (Sapozhnikov et al. 2012). It has a dark-blue color, and its framework is topologically identical to the frameworks of minerals of the sodalite group, although the unit cell volume is six times larger than the unit cell volume of cubic lazurite. It is noteworthy that the charge balance in the vladimirivanovite formula can be achieved only on the condition that sulfide sulfur forms radical anion (S₃)⁻.

As noted earlier, the ideal formula of lazurite is Na₆Ca₂[Al₆Si₆O₂₄]S₂, where S is the S²⁻ anion. However, Hassan et al. (1985) were unable to explain the amount of sulfur, often exceeding 2 atoms per formula unit, which may violate the electroneutrality of the formula. To solve this problem, Hogarth and Griffin (1976) proposed that excess sulfur occurs within the framework, partially replacing oxygen atoms.

Taylor (1967) measured the superstructural periodicity of nine sulfate-enriched sodalites and found their superstructure to be incommensurate according to the satellite reflections in the X-ray diffraction (XRD) patterns. In nosean, haüyne, and lazurite containing tetrahedral anions of (SO₄)²⁻, the ordering of clusters of different sizes causes modulation of the displacement of the oxygen atoms in the framework, resulting in superstructural reflections appearing in diffraction patterns (Hassan and Buseck 1989). In non-cubic varieties of lazurite, the commensurate superstructure can be caused by modulation of the displacement of AlO₄ and SiO₄ tetrahedra from their positions in the cubic mineral (Evsyugin et al. 1997, 1998). Commensurability or incommensurability of the superstructure is estimated by the value of the satellite displacement from the main reflection along the axis of the reciprocal lattice. If the displacement fits between the main reflections an integer number of times, the superstructure is commensurate; otherwise, it is incommensurate. Satellite displacement (structure modulation parameter) may be different in different samples. In optically isotropic cubic lazurite

samples, the value of the incommensurate modulation parameter varies from 0.169 to 0.217 (Sapozhnikov 1992). According to Bolotina (2006), incommensurate modulation in lazurite is due to the alternation of three-dimensional areas of diverse volumes in its structure.

The aim of this work was to study the properties and chemical composition and to specify the crystal-chemical formula of S-rich lazurite using a combination of mineralogical, chemical, and physical analytical methods. In the study, two samples (Fig. 1) of dark blue lazurite with high sulfur contents were collected from the Malo-Bystrinskoe lazurite deposit (Baikal Lake area, Russia). The samples are structurally unique among lazurites from different locations and differ from them by the incommensurate modulation parameter equal to 0.147.

GEOLOGICAL SETTING AND PETROLOGICAL DATA

Rocks with high-sulfur lazurite are lenticular metasomatic bodies ranging in size from 4 × 7 cm to 15 × 30 cm (sample 1) and lazurite-containing calciphyres (sample 2). In sample 1, the lazurite contained varying amounts of subordinate forsterite, pyroxene, and calcite. This type of rock is rare for the Malo-Bystrinskoe deposit. The second sample was lazurite-containing calciphyre with minor bystrite. Both rocks were confined to dolomite marbles.

The lazurite-dominant rocks (sample 1) have a taxitic structure due to the irregular accretion of dark blue lazurite among white calcite, diopside, forsterite, and rare phlogopite. Lazurite aggregates were composed of dark blue single-crystal individuals ranging in size from 0.2 to 5 mm with perfect cleavage. The mineral content (wt%) in the rock was: phlogopite, up to 10; forsterite, 5–20; pyroxene, 5–30; calcite, 40–60; and lazurite, 60–95. This type of rock is an apocarbonate lazurite metasomatite, developed within early forsterite, pyroxene, and forsterite-pyroxene skarns of the magmatic stage. This was evidenced by observations in thin sections: grains of forsterite and pyroxene were corroded by lazurite and phlogopite and were present as relics of different shapes in poikiloblasts

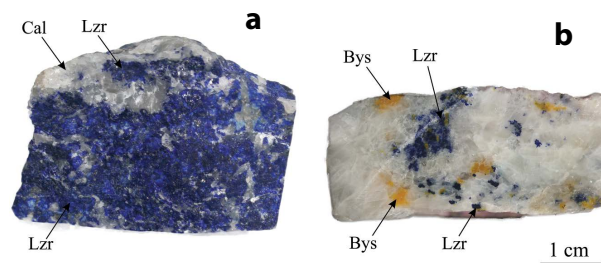


FIGURE 1. Samples of rocks with high-sulfur lazurite: (a) lenticular body (sample 1), (b) lazurite-containing calciphyre with bystrite (sample 2). Abbreviations: Lzr = lazurite, Bys = bystrite, Cal = calcite.

of lazurite; moreover, some lazurite crystals formed as a result of recrystallization and do not contain inclusions. Small relic grains of dolomite are dispersed randomly in calcite aggregates in amounts up to 3 wt%. In addition, grains of corroded pyrite were observed in lazurite-bearing metasomatic rocks. The early generation of calcite is represented by individual grains (0–7%) represented by calcite syngenetic with lazurite, which forms coarse crystals and irregular scalloped edges of granules. Lazurite, in addition to forsterite and diopside inclusions, may contain early skeletal (graphic, diablast) pyroxene-lazurite accretions 2–6 mm in size.

Polycrystalline aggregates of lazurite can reach several centimeters across and, as a rule, are the later products of early lazurite recrystallization. In general, the dominating metasomatic structure is heterogranoblastic, with areas of microdiablastic structures containing varying amounts of diopside, forsterite, calcite, and lazurite in the form of individual grains and their intergrowths.

The second type of rock (sample 2) is represented by lazurite-containing calciphyres, dominated by calcite (70–80%). Forsterite and pyroxene (5–10% each), lazurite (10–15%), bystrite (1–3%), and minor phlogopite are also present. These rocks are characterized by a very irregular distribution of silicates and aluminosilicate minerals, including lazurite. Bystrite occurs in lazurite-containing calciphyres as pseudomorphs after lazurite grains.

In transmitted light, both samples of S-rich lazurite have a saturated dark blue color with different shades that is virtually uniform within each individual sector. Their “velvet” color differs from the usual blue color of lazurite with deeper intensity. Observations in cross-polarized light (in crossed nicols) in one-third of the cases demonstrated near complete extinction with dark brown tints. The absence of complete extinction indicates slightly non-isotropic optical properties. In some cases, abnormal color with dark gray shades was observed in cross-polarized light.

It should be noted that the X-ray diffraction patterns of samples 1 and 2 near the lines of lazurite showed weak lines of sodalite, although sodalite was not observed in the thin section. However, the presence of sodalite forming thin zones (up to 10 μm) around lazurite grains as well as in cracks in lazurite (together with calcite) was detected by characteristic X-ray radiation of Cl. It is evident that the surficial substitution of lazurite by sodalite occurred under the action of late fluid deficient in sulfur and enriched in NaCl.

The rocks studied formed after the carbonate substrate, in some areas with complete replacement of early diopside-forsterite-containing metasomatites. This differs from the usual method of formation after aluminosilicate (granite, syenite, nepheline syenite) substrates. In thin sections of both rock types with high-S lazurite, we observed net-like (graphic) lazurite structures in calcite, as well as replacement of forsterite and diopside by lazurite and formation of diablastic intergrowths of diopside with lazurite in the carbonate substrate.

METHODS OF STUDY

Chemical composition

The samples of lazurite were studied on a JXA_8200 JEOL electron microprobe equipped with a high-resolution scanning electron microscope, an energy-dispersion system (EDS), a SiLi detector with a resolution of 133 eV, and five wave-dispersion spectrometers (WDS). The chemical composition was measured with WDS operated at an acceleration voltage of 20 kV, with a current intensity of 10 nA and a counting time of 10 s. The beam was defocused to 20 μm to decrease the thermal effect on the sample. Under these conditions, the mineral was stable

with respect to the beam effect.

The following standards and analytical lines were used: pyrope (Si, $K\alpha$), albite (Al, Na, $K\alpha$), diopside (Ca, $K\alpha$), orthoclase (K, $K\alpha$), barite (S, $K\alpha$), and Cl-apatite (Cl, $K\alpha$). The contents of the elements were calculated using the ZAF procedure. Quantitative analyses of 30 local areas in sample 1 and 30 local areas in sample 2 were conducted. The compositions of six grains were measured for each sample; the intensities of analytical lines were measured at five points in each grain. The relative standard deviation characterizing reproducibility of the measurement of the determined element and chemical homogeneity of the samples did not exceed 1.3% for Al and Si; 2% for Na, S, and Ca; or 3% for Cl and K, which indicates the regular distribution of mineral-forming elements in lazurite. The backscattered images obtained by scanning sample areas did not reveal sulfide inclusions (FeS₂, FeS).

Electron microprobe analysis (EMPA) was used to determine the total sulfur content in the samples. Sulfate sulfur in sample 1 was determined by conventional wet chemical analysis using acidic decomposition. Sulfide sulfur was accepted as the difference between the total sulfur and the sulfate sulfur.

Thermoanalytical study

Thermal analysis was performed on a synchronous thermal analyzer (STA 449 F1 Jupiter). Control of the composition of the gaseous thermolysis products was carried out using a quadrupole mass spectrometer (QMS 403 C Aëolos), with the energy of electron impact set at 70 eV. Over the course of sample heating, the tool enables simultaneous acquisition of data regarding changes in the sample weight, the rate of weight change, the thermal effects in the system, and the composition of the released gaseous phase. The thermal data were obtained in an argon atmosphere, in the temperature range from 20 to 1400 °C, at a heating rate of 5 °C/min.

Spectroscopic study

The infrared absorption spectra of high-S lazurite were measured by Fourier-transform IR spectroscopy (FTIR) using an FT-801 spectrometer (Simex, Russia) and ALPHA FTIR spectrometer (Bruker Optics). Powdered samples were mixed with anhydrous KBr, pelletized, and analyzed at a resolution of 4 cm^{-1} . A total of 16 scans were collected in the wavenumber range 360 to 3800 cm^{-1} . The IR spectrum of an analogous pellet of pure KBr was used as a reference.

Lazurite dehydration was conducted as follows. Lazurite and KBr were ground in a mortar, kept at a given temperature for 10 min in a muffle furnace, and then cooled to room temperature. Thereafter, two tablets were pressed, one from a mixture of lazurite and KBr and another one (reference sample) from pure KBr. The IR spectrum of the latter was subtracted from the spectrum of the sample with lazurite. Next, powders of both samples were heated to the next temperature in the interval from 25–600 °C, and the procedure was repeated. Tablets were prepared and absorption spectra were measured under conditions of low relative humidity (<20%); therefore, water adsorption in heated samples can be neglected.

The Raman spectrum of a randomly oriented S-rich lazurite sample was obtained using an EnSpectr R532 spectrometer based on an OLYMPUS CX 41 microscope coupled with a diode laser ($\lambda = 532 \text{ nm}$) at room temperature. The spectrum was recorded in the range of 100 to 4000 cm^{-1} with a diffraction grating of 1800 gr mm^{-1} and a spectral resolution of 6 cm^{-1} . The output power of the laser beam was 5 mW. The diameter of the focal spot on the sample was <5 μm . The backscattered Raman signal was collected with a 40 \times objective; signal acquisition time for a single scan of the spectral range was 1 s, and the signal was averaged over 50 scans. Crystalline silicon was used as the standard.

The EPR experiment was performed on the lazurite using an X-band spectrometer RE1306 operated at a microwave frequency of 9380 MHz. The spectrometer was equipped with a cryostat operated at temperatures down to 77 K.

The XPS spectra were obtained with a SPECS instrument (SPECS, Germany) equipped with a PHOIBOS 150 MCD-9 hemispherical electron energy analyzer. The spectra were acquired at excitation initiated by monochromated AlK α (1486.74 eV) radiation with a power of 220 W and voltage at the tube of 12.5 kV. The high-resolution spectrum of S 2p (narrow scan) was recorded with a 0.05 eV interval and transmission energy of 8 eV. Lazurite sample 1 was powdered to a mean particle size of 0.01–0.02 mm immediately before placing it in the analysis chamber. The surface of the sample was not purified by ion etching. This is important in the study of lazurite because etching by Ar⁺ causes a reduction of sulfate sulfur. The C 1s peak at 285 eV from natural hydrocarbon contaminants was used to correct the binding energies (BE) for the surface charging. The 2p sulfur spin-orbital doublet was unfolded and fitted by CasaXPS software after subtracting the nonlinear background by Shirley's method and taking into account separation of the doublet components S 2p_{3/2} and S 2p_{1/2} equal to 1.2 eV and the proportion of their intensities as 2:1. The peak shapes were described by the Voigt function

(i.e., convolution of Gauss and Lorentz functions). Peak attribution was performed according to data published previously (Tauson et al. 2012). The accuracy of the BE was estimated to be ± 0.1 eV.

X-ray diffraction study

The X-ray diffraction study was carried out by the photo method on a single crystal (RKV-86 camera, $\text{CuK}\alpha$ +beta radiation) and the powder diffraction method with an automatic powder diffractometer (D8 ADVANCE, Bruker, Germany) equipped with a Göbel mirror. The powder X-ray diffraction patterns were obtained in step scan mode (in the 2θ range of 5 to 70°), using $\text{CuK}\alpha$ radiation, at an accelerating voltage of 40 kV, current of 40 mA, time per step of 1 s, and 2θ step of 0.02°. The calculations of interplanar distances and intensities of diffraction lines were performed using the computational software that was delivered with the diffractometer (DIFFRAC Plus Evaluation package EVA, Bruker AXS). The description of the modulated structure was carried out using a previously published scheme (Sapozhnikov 1992) with the modulation parameter estimated in the present work. The dependence of the unit-cell parameter on temperature for a sample heated up to 750 °C in air was calculated based on the position of the 440 line, which was measured in situ in the course of heating a sample placed on the camera of the diffractometer using a high-temperature cell NTK 16.

RESULTS AND DISCUSSION

Chemical composition and formula of lazurite

According to the electron microprobe analyses (Table 2), the total content of sulfur in the S-rich lazurite (sample 1) was 8.30 wt%. According to the wet chemistry studies performed, the mineral contained sulfate sulfur in the amount of 3.23 wt% S^{6+} , which corresponds to 8.08 wt% SO_3 . The amount of sulfide sulfur was calculated as the difference between total sulfur and sulfate sulfur and was equal to 5.07 wt%.

The empirical formula based on 12 (Si+Al) atoms per formula unit under the assumption that all sulfide sulfur is present in the form of S^{2-} (in accordance with the standard lazurite formula given in the IMA list of minerals) is $(\text{Na}_{6.97}\text{Ca}_{0.88}\text{K}_{0.10})_{7.95}[\text{Al}_{5.96}\text{Si}_{6.04}]_{12}\text{O}_{24}(\text{SO}_4)_{1.09}(\text{S}^{2-})_{1.71}\text{Cl}_{0.04}\cdot 0.72\text{H}_2\text{O}$. This formula is unbalanced in charge, with the sums of cations and anions equal to +50.87 and -53.64 charge units, respectively. However, sulfur atoms are known to be present in the structure of lazurite in the form of radical ions, such as $(\text{S}_2)^{\cdot-}$ and $(\text{S}_3)^{\cdot-}$ (Platonov et al. 1971; Clark et al. 1983; Gobeltz-Hautecoeur et al. 2002). To achieve electroneutrality, 1.71 sulfide sulfur atoms should be combined

TABLE 2. Chemical composition of high-sulfur lazurite (samples 1 and 2) and stoichiometric coefficients for the components calculated on (Al + Si) = 12 atoms per formula unit

Component	Mean content		Range		Atom / group	Formula coefficient	
	1	2	1	2		1	2
SiO_2	33.48	33.15	34.33–32.35	33.64–31.64	Si	6.04	6.01
Al_2O_3	28.02	28.06	28.33–27.64	28.70–27.41	Al	5.96	5.99
CaO	4.56	4.35	4.79–4.13	4.94–4.22	Ca	0.88	0.85
Na_2O	19.94	20.27	20.57–19.00	20.98–18.72	Na	6.97	7.12
K_2O	0.43	0.04	0.53–0.31	0.10–0.02	K	0.10	0.01
Cl	0.13	0.02	0.21–0.07	0.06–0.01	Cl	0.04	0.02
SO_3	8.08 ^a	7.35 ^c			SO_4	1.09	1.00 ^c
S	5.07 ^b	7.23 ^b			S_3	0.55	0.82 ^c
					S	0.05	–
H_2O	1.2	n.d.			H_2O	0.72	n.d.
–O=S	–0.42	–0.60					
–O=Cl	–0.03	0					
Total	100.46	99.87					

Notes: n.d. = not determined. –O=S is calculated for $(\text{S}_3)^{\cdot-}$.

^a Determined by wet chemical analysis.

^b Calculated as the difference between total sulfur and sulfate sulfur.

^c Calculated based on the charge-balance condition; all sulfide sulfur in sample 2 was considered $(\text{S}_3)^{\cdot-}$.

into groups with a total charge of -0.65. This is possible only under the assumption that part of the sulfide sulfur belongs to the trisulfide radical anion because all other variants result in excess negative charge. On the other hand, the assumption that $(\text{S}_3)^{\cdot-}$ is the only form of sulfide sulfur in S-rich lazurite leads to a deficit of negative charge.

Table 3 shows different variants of combining sulfide sulfur atoms, which result in electroneutrality of the empirical formula. All combinations resulted in a significant dominance of the trisulfide radical anion over other forms of sulfide sulfur. Despite the fact that all combinations given in Table 3 agree with the chemical data and the charge balance requirement, only variant no. 1 is acceptable because Raman and XPS data exclude all sulfide anions except $(\text{S}_3)^{\cdot-}$ and S^{2-} (Table 3).

Samples 1 and 2 have similar contents of most components (Table 2), but differ in total sulfur content (8.30 wt% in sample 1 and 10.17 wt% in sample 2). Unfortunately, we were unable to determine the amount of sulfate sulfur in sample 2 by chemical methods due to the lack of pure material. Calculation of the formula under the assumption that the number of Ca atoms is equal to the number of SO_4 groups (in accordance with crystal-chemical considerations, see below), showed that $(\text{S}_3)^{\cdot-}$ is the predominant form of sulfur in sample 2 (Table 2). The mineral contained more sulfide than sulfate sulfur, which is a distinctive feature among lazurites from the Baikal Lake area.

The formulas of the samples were balanced in charge, emphasizing the fact that sulfide sulfur in lazurite was represented mainly by the radical ion $(\text{S}_3)^{\cdot-}$, the presence of which is in agreement with the dark blue color of the mineral and confirms the conclusion that “the connection of the blue color (of lazurites) with the radical $(\text{S}_3)^{\cdot-}$ is ... an indisputable fact” (Platonov et al. 1971).

The ideal chemical formula for S-rich lazurite is $\text{Na}_7\text{Ca}[\text{Al}_6\text{Si}_6\text{O}_{24}]\text{SO}_4(\text{S}_3)^{\cdot-}\cdot\text{H}_2\text{O}$, and in comparison with the idealized formula of nosean $\text{Na}_8[\text{Al}_6\text{Si}_6\text{O}_{24}]\text{SO}_4\cdot\text{H}_2\text{O}$ and haüyne $(\text{Na},\text{K})_6\text{Ca}_2[\text{Al}_6\text{Si}_6\text{O}_{24}](\text{SO}_4)_2$, reveals the difference in the charge value of the extra-framework cations. In nosean, it equals +8. In the mineral under study, it equals +9, and in haüyne, it is +10 charge units. It should be noted that sulfate-free lazurite with the idealized formula $[\text{Na}_6\text{Ca}_2[\text{Al}_6\text{Si}_6\text{O}_{24}](\text{S}^{2-})_2]$ has not been found in nature. However, Tauson et al. (1998) synthesized such a compound, so-called “S-sodalite,” as a product of annealing of lazurite at 800 °C and low fugacity of SO_2 in the gaseous phase. This compound has gray color and a unit-cell parameter of 8.944 Å, which is close to the *a* parameter of sodalite (Table 1).

Thermal analysis

A comparison of thermogravimetric (TG) and differential scanning calorimetry (DSC) data (Fig. 2) with ion currents corresponding to different mass numbers led us to conclude

TABLE 3. Different variants incorporating 1.7 atoms of sulfide sulfur into the lazurite structure under the assumption that the total charge is equal to -0.65

Variant no.	Amount of different sulfide ions	Charge of formula
1	$(\text{S}_3)_{0.55} + (\text{S}^{2-})_{0.05}$	-0.65
2	$(\text{S}_2)_{0.53} + (\text{S}_2)_{0.06}^{\cdot-}$	-0.65
3	$(\text{S}_3)_{0.49} + (\text{S}_2)_{0.08}^{\cdot-}$	-0.65
4	$(\text{S}_2)_{0.41} + (\text{S}_2)_{0.24}^{\cdot-}$	-0.65

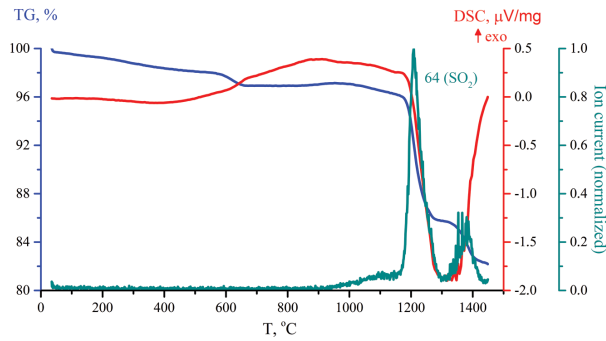


FIGURE 2. Thermogravimetric (TG) and differential scanning calorimetry (DSC) curves and the temperature dependence of the SO_2 ion current (mass number 64) for lazurite sample 1.

that endothermic effects observed in the temperature ranges 300–550 (I), 550–670 (II), 960–1300 (III), and 1300–1450 °C (IV) and accompanied by a 1.2, 3.1, 11.4, and 3.5% weight loss were due to the release of H_2O (I), CO_2 (II), and SO_2 (III and IV) as a result of oxidation of sulfide groups (III), and SO_2 evolved from sulfate groups (IV), respectively.

Raman spectroscopy

Raman spectroscopy is a sensitive tool used to detect trisulfide anion radicals because Raman bands characteristic of $(\text{S}_3)^-$ are strong (Climent-Pascual et al. 2009). Figure 3 shows the Raman spectrum of S-rich lazurite. Raman shifts (cm^{-1}), band intensities (s for strong, m for medium, and w for weak), and assignment of bands are shown in Table 4.

The assignment of bands was made in accordance with Reshetnyak et al. (1986), Steudel (2003), Tossell (2012), and Chivers and Elder (2013).

It is important to note that S^{2-} is the only sulfide anion that does not have internal vibrations. Bands of other sulfide anions, except those of S_3^- , were absent in the Raman spectrum of S-rich lazurite. This fact confirms the conclusion that only three kinds of S-bearing anions were present in sample 1: S_3^- , S^{2-} , and $(\text{SO}_4)^{2-}$.

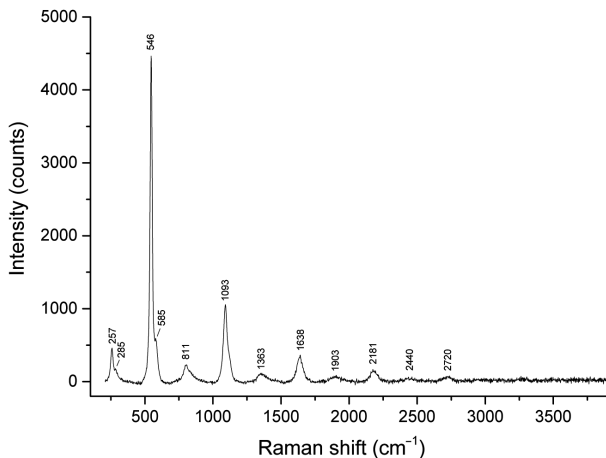


FIGURE 3. Raman spectrum of S-rich lazurite (sample 1).

TABLE 4. Raman spectrum characteristics of S-rich lazurite

Raman shift (cm^{-1})	Intensity	Assignment of bands
257	m	ν_2 (A_2) of S_3^- – bending vibrations
285	w	combination of lattice modes
546	s	ν_1 (A_1) of S_3^- – stretching vibrations
585	m	ν_4 of SO_4^{2-} – bending vibrations
811	w	combination mode $\nu_1 + \nu_2$ of S_3^-
988	w	ν_2 of SO_4^{2-} – symmetric stretching vibrations
1093	s	overtone $2\nu_1$ of S_3^-
1363	w	combination mode $2\nu_1 + \nu_2$ of S_3^-
1638	m	overtone $3\nu_1$ of S_3^-
1903	w	combination mode $3\nu_1 + \nu_2$ of S_3^-
2181	w	overtone $4\nu_1$ of S_3^-
2440	w	combination mode $4\nu_1 + \nu_2$ of S_3^-
2720	w	overtone $5\nu_1$ of S_3^-

Infrared spectroscopy

The strongest bands in the IR spectrum of S-rich lazurite (Fig. 4) were observed at 1000 cm^{-1} and in the ranges of $600\text{--}720$ and $380\text{--}500 \text{ cm}^{-1}$ that correspond to stretching, mixed, and bending modes of the tetrahedral framework, respectively. The band at 3420 cm^{-1} is due to O-H stretching vibrations of H_2O molecules. Two bands of nondegenerate bending vibrations of H_2O (at 1622 and 1683 cm^{-1}) indicate the presence of two kinds of locally non-equivalent water molecules in the β -cages of S-rich lazurite. The band at 2342 cm^{-1} corresponds to antisymmetric stretching vibrations of admixed CO_2 molecules (Bellatreccia et al. 2009; Balassone et al. 2012).

As compared with the IR spectra of haüyne and nosean, the spectrum of S-rich lazurite is characterized by lowered intensities in the bands of asymmetric S-O stretching vibrations of $(\text{SO}_4)^{2-}$ anions (in the range $1090\text{--}1150 \text{ cm}^{-1}$) and the presence of an additional band at 580 cm^{-1} associated with antisymmetric stretching vibrations in $(\text{S}_3)^-$ anions (ν_3 mode: Clark and Cobbold 1978; Wong 2003; Li et al. 2011; Chivers and Elder 2013) that confirms the content of $(\text{S}_3)^-$ anions in the sample. Climent-Pascual et al. (2009) suggested that $(\text{S}_3)^-$ anions can occupy up to 15% of the β -cages in the mineral structure.

Figure 5 shows the temperature dependence of the absorption band intensity in the region of 3400 cm^{-1} that was obtained by measuring the optical density corresponding to the absorption maximum; absorbance at 3200 cm^{-1} was used as background. The absorption of lazurite, which was not subjected to thermal

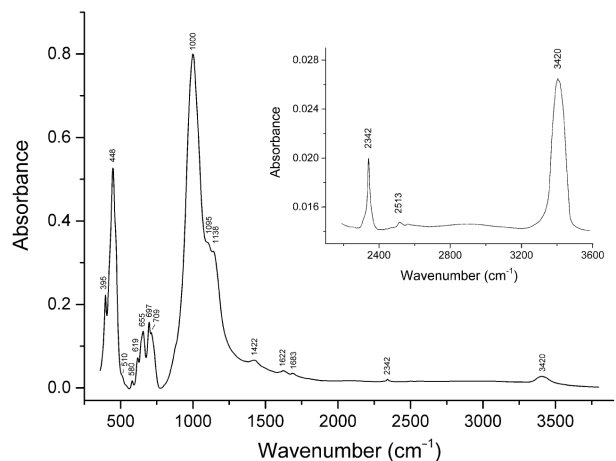


FIGURE 4. Infrared absorption spectrum of S-rich lazurite (sample 1).

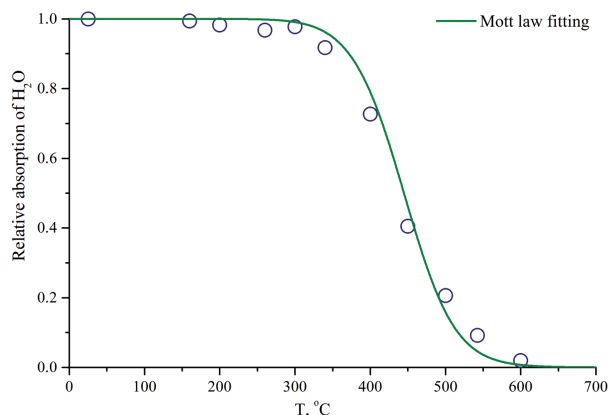


FIGURE 5. Temperature dependence as a function of relative intensity of IR absorption at 3400 cm^{-1} (stretching vibrations of H_2O molecules).

treatment, was accepted as equal to one. The most intense release of H_2O was observed in the temperature range of $350\text{--}550\text{ }^\circ\text{C}$. Absorption spectra in the IR region show that the lazurite samples were close to the previously synthesized ultramarine-type lazurites (Arieli et al. 2004; Gesing and Buhl 1998; Fechtelkord 1999; Climent-Pascual et al. 2009).

EPR spectroscopy

The EPR spectrum of S-rich lazurite is shown in Figure 6. One broad line was observed at $g = 2.030$. This signal was previously associated with the $(\text{S}_3)^{\cdot-}$ radical anion (Pinon et al. 1992). The g factor of $(\text{S}_3)^{\cdot-}$ is greater than that of a free electron, which corresponds to the model of the $(\text{S}_3)^{\cdot-}$ center with an electron and a hole on the outer shell of the anion.

X-ray diffraction

The X-ray diffraction patterns of sample 1 contain basic and superstructural reflections (Table 5). Basic reflections define the primary cubic sub-cell with the parameter $9.087(3)\text{ \AA}$ and space group $P43n$.

Superstructural reflections of two types correspond to the commensurate and incommensurate superstructure (Fig. 7). No

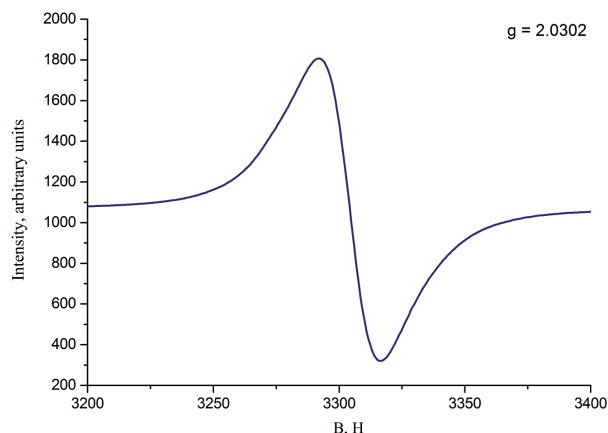


FIGURE 6. EPR spectrum of S-rich lazurite at room temperature.

reflections of admixed sodalite were observed in the single-crystal X-ray rotation photographs. The $[100]$ X-ray rotation photograph of a crystal (Fig. 8) demonstrated a small number of reflections of commensurate superstructure lying in the middle of the basic reflection arrays (these reflections correspond to the lines at 4.867 , 3.117 , 2.948 , 1.9604 , and 1.7013 \AA in Table 5). The incommensurate superstructure is registered by the position of the satellites of the main reflections. Numerous satellites of the first order on the rotation radiograph look like arrays located above and below the rows of basic reflections. Analysis of the diffraction pattern showed that the distribution scheme of satellites characterizing the sample was the same as for previously studied lazurites from the Baikal Lake area and Southwestern Pamir (Sapozhnikov 1992). The difference was in the magnitude of the structure modulation parameter, which was determined by the satellite displacement from the basic reflections along the reciprocal lattice axis. The parameter n was determined from the lazurite single-crystal X-ray rotation photograph (Fig. 8) and refined using the symmetric satellites at the strong basic lines 211, 222, and 411 in the powder diffraction pattern (Table 5) using the following expressions:

$$n = \frac{a^2}{12} \left(\frac{1}{d_{2+n,1+n,1}^2} - \frac{1}{d_{2-n,1-n,1}^2} \right), \quad n = \frac{a^2}{8} \left(\frac{1}{d_{2,1+n,1+n}^2} - \frac{1}{d_{2,1-n,1-n}^2} \right),$$

$$n = \frac{a^2}{16} \left(\frac{1}{d_{2+n,2+n,2}^2} - \frac{1}{d_{2-n,2-n,2}^2} \right), \quad \text{and} \quad n = \frac{a^2}{12} \left(\frac{1}{d_{4+n,1-n,1}^2} - \frac{1}{d_{4-n,1+n,1}^2} \right).$$

The refined n value of 0.1479 was put into quadratic form for cubic crystals.

TABLE 5. Powder X-ray diffraction data of high-sulfur lazurite (sample 1)

hkl^a	D_{meas}	D_{calc}	l	hkl^a	D_{meas}	D_{calc}	l
110	6.437	6.426	18.4	$1+n,1+n,4$	2.111	2.105	3.7
$2-0.5,1-0.5,1$	4.867	4.857	6.7	$4+n,1-n,1$	2.091	2.089	5.8
200	4.548	4.544	8.3	$4+n,1+n,1$	2.057	2.057	3.3
210	4.067	4.064	4.7	$4+0.5,1-0.5,1$	1.9604	1.9598	3
$2-n,1-n,1$	4.009	4.001	4.5	332	1.9367	1.9374	3.7
$1-n,1-n,2$	3.895	3.891	4.4	$3+n,2+n,3$	1.8736	1.8739	3
211	3.711	3.710	100	$2+n,2-n,4$	1.8543	1.8533	2.7
$1+n,1+n,2$	3.530	3.528	5.3	510	1.7821	1.7822	9.4
$2+n,1+n,1$	3.450	3.453	4.6	$4+n,1+n,3$	1.7329	1.7323	2.6
220	3.211	3.213	4.3	$3+0.5,3+0.5,2$	1.7013	1.7022	2.5
$2-0.5,1+0.5,1$	3.117	3.117	7.3	521	1.6592	1.6591	3.4
$2+0.5,1+0.5,1$	2.948	2.948	4.7	$4-n,0+n,4$	1.6355	1.6357	2.6
310	2.875	2.874	16.3	440	1.6063	1.6064	7.2
$2-n,2-n,2$	2.761	2.757	4.8	433	1.5585	1.5585	4.2
222	2.623	2.623	29.5	442	1.5144	1.5146	3.8
$3-n,2-n,1$	2.564	2.563	4.2	532	1.4744	1.4742	4.8
$2+n,2+n,2$	2.499	2.499	4.5	$6+n,0+n,2$	1.4027	1.4054	2
321	2.428	2.429	7	$6-n,2+n,2$	1.3879	1.3880	2.1
$3+n,1-n,2$	2.372	2.376	3.9	622	1.3702	1.3700	5.6
$2+n,1+n,3$	2.349	2.352	3.4	631	1.3399	1.3399	2.4
$3+n,2+n,1$	2.308	2.307	3.6	444	1.3116	1.3116	3.8
400	2.272	2.272	8.3	550	1.2855	1.2851	2.5
$4-n,1-n,1$	2.236	2.232	4.1	$5+2n,5-2n,0$	1.2827	1.2829	2.3
$4-n,1+n,1$	2.194	2.194	3.7	$5+n,0+n,5$	1.2655	1.2661	1.9
411	2.142	2.142	15.7	721	1.2369	1.2366	3.8

Note: The sub-cell parameter $a = 9.087(3)\text{ \AA}$ and $n = 0.147$.

^a Simple symbols (110, etc.) denote the indices of basic reflections; symbols containing ± 0.5 ($2-0.5,1-0.5,1$, etc.) refer to the powder diffraction lines of commensurate superstructure; symbols ($h\pm n, k\pm n, l$)—containing n , the parameter of the incommensurate modulation—refer to the lines of incommensurate superstructure (satellite reflections).

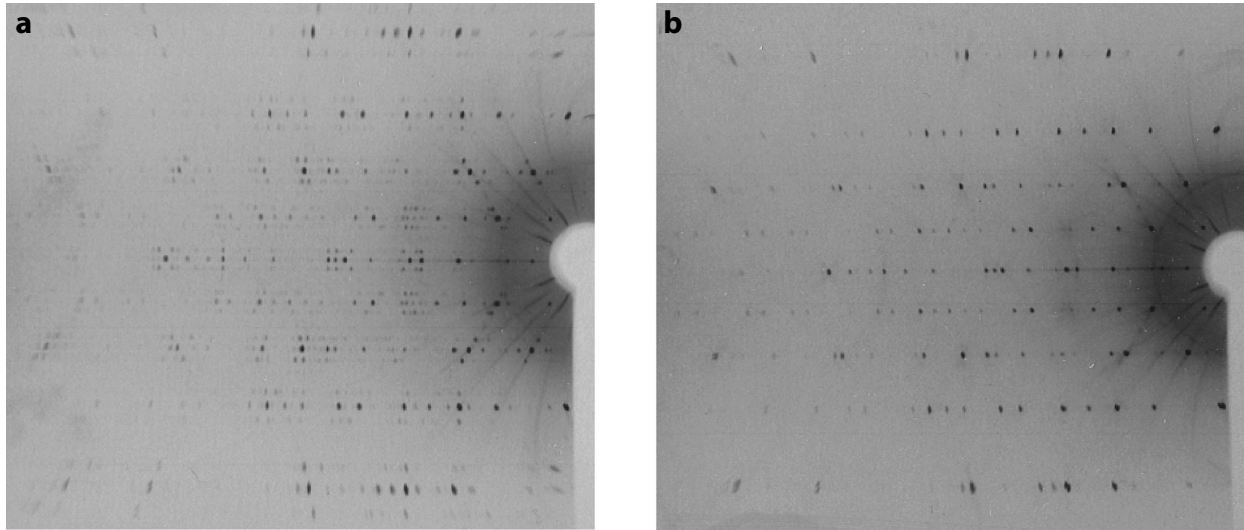


FIGURE 7. Single-crystal X-ray rotation photographs of lazurite ($a = 9.071 \text{ \AA}$ and $n = 0.218$): initial crystal of lazurite with (a) incommensurate modulation reflections and (b) crystal annealed at $650 \text{ }^\circ\text{C}$ in air for 1 h, without incommensurate modulation reflections.

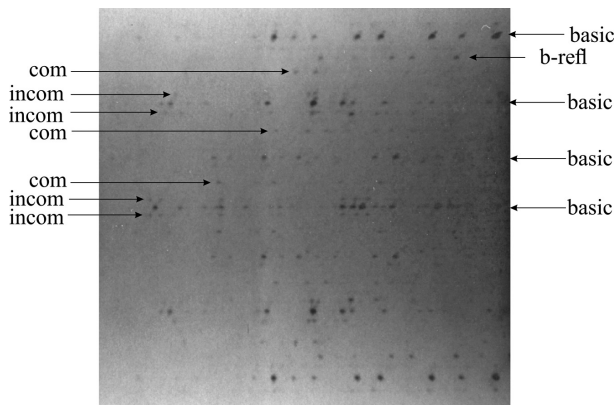


FIGURE 8. The [100] single-crystal X-ray rotation photograph of S-rich lazurite (sample 1). basic = reflections of the subcell; com = commensurate modulation; incom = incommensurate modulation; and b-refl = β -reflections are indicated.

$$\frac{1}{d_s^2} = \frac{(h \pm n)^2 + (k \pm n)^2 + l^2}{a^2}$$

where d_s is the interplanar spacing of a satellite, a is the basic sub-cell parameter, and hkl are the indices of the main sub-cell reflection near which the satellite under consideration was located. After that, we determined the d -spacings of other satellites using the exhaustive search and Microsoft Excel software.

Half of the total number of lines in Table 5 correspond to incommensurate satellites. The low value of the reliability index $R = (\sum |d_{\text{meas}} - d_{\text{calc}}|) P^{-1} = 0.002 \text{ \AA}$ (where P is the total number of satellites) shows the invariability of the incommensurate displacement of all satellites from the basic reflections. After annealing the mineral in air at $750 \text{ }^\circ\text{C}$, the modulation disappeared, and the sub-cell parameter increased to $9.107(3) \text{ \AA}$. The parameter was estimated from the powder X-ray diffraction pattern of the sample cooled to room temperature, after sample repacking.

Figure 9 shows the dependence of the sub-cell parameter on the annealing temperature in air. The graphs reflect the change in the coefficient of thermal expansion (compression) of lazurite during annealing and cooling. In the range of 30 to $550 \text{ }^\circ\text{C}$, the coefficient of thermal expansion $\alpha_1 = 1.87 \cdot 10^{-5} \text{ K}^{-1}$. In the interval 550 – $600 \text{ }^\circ\text{C}$, it decreased to near zero ($\alpha_2 = 7.19 \cdot 10^{-7} \text{ K}^{-1}$). It should be noted that according to IR spectroscopy data, the interval 550 – $600 \text{ }^\circ\text{C}$ corresponds to the completion of water release during heating. In the range of 600 to $750 \text{ }^\circ\text{C}$, the mineral begins to expand again, but to a lesser extent than the first time, and $\alpha_3 = 5.54 \cdot 10^{-6} \text{ K}^{-1}$.

The irregular change in the sub-cell parameter indicates a change in the thermal expansion mechanism. In the first stage, the expansion proceeds through a simultaneous unfolding of the AlO_4 and SiO_4 tetrahedra according to the mechanism proposed by Pauling (1930) for sodalite. Thermal expansion above $600 \text{ }^\circ\text{C}$ is caused by a small change in the average distance between the atoms in the framework as the kinetic energy increased. The mismatch in the sub-cell parameters of the initial and annealed mineral at $30 \text{ }^\circ\text{C}$ (hysteresis) may be due to partial oxidation of sulfide sulfur under annealing. The parameter of the sub-cell (a), the modulation parameter (n), and the period of incommensurate modulation of the structure (T_m) are related by the equation $a = nT_m$. In the studied mineral, the period of incommensurate modulation equaled 61.82 \AA . In the structure of the common cubic lazurite ($a = 9.071 \text{ \AA}$ and $n = 0.218$) from the Baikal Lake area, it equals 41.61 \AA (Ivanov and Sapozhnikov 1985; Tauson et al. 1998).

X-ray photoelectron spectroscopy

Figure 10 shows the X-ray photoelectron spectrum of the high-S lazurite sample 1. The BEs and concentration of S-bearing groups are presented in Table 6.

Two sulfur species, sulfate sulfur and polysulfide sulfur, were detected by means of XPS. The mole ratio of $(\text{S}_3)^-$ to $(\text{SO}_4)^{2-}$ was 0.35 , which is somewhat lower as compared to the previously calculated value of 0.5 (Table 2). The possible cause of this dis-

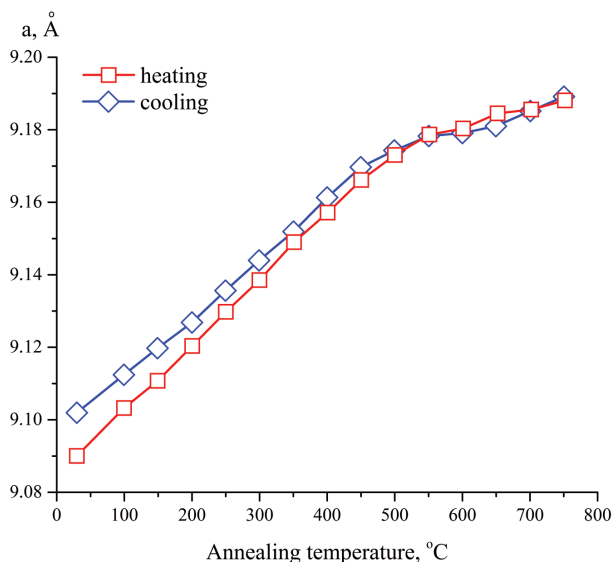
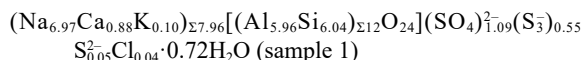


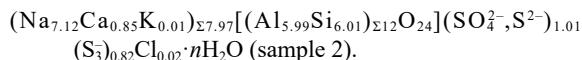
FIGURE 9. Dependence of the sub-cell parameter of S-rich lazurite on temperature.

crepancy is partial oxidation of sulfur during sample preparation. Nevertheless, the data obtained support the idea that lazurite, being a mineral containing the trisulfide radical anion (S_3^-), was detected in the XPS spectrum as the only polysulfide species incorporated into the structure of high-S lazurite together with sulfate anions. The monosulfide anion S^{2-} was not detected in the S 2p spectrum because of its low content (Table 3) and easy oxidation in powdered form when used for XPS (Tauson et al. 2012).

Based on the combination of chemical, IR, Raman, EPR, and XPS data, the charge-balanced empirical formulas calculated on 12 (Al+Si) atoms per formula unit can be written as follows:



and



Thus, the idealized formula of S-rich lazurite is $\text{Na}_7\text{Ca}[\text{Al}_6\text{Si}_6\text{O}_{24}](\text{SO}_4)^{2-}(\text{S}_3^-) \cdot n\text{H}_2\text{O}$. It refers to two types of clusters, $[\text{Na}_3\text{Ca} \cdot \text{SO}_4]^{3+}$ and $[\text{Na}_4(\text{S}_3)]^{3+}$, that occupy structural cages in equal proportion.

IMPLICATIONS

The ideal crystal-chemical formula of lazurite $\text{Na}_6\text{Ca}_2[\text{Al}_6\text{Si}_6\text{O}_{24}]\text{S}_2$, as recommended in the IMA list of minerals (see Introduction), differs from the ideal formula of lazurite obtained in this work. The difference is of principal value. The “ideal” formula suggests only one kind of sulfur species and one position of sulfur in the lazurite structure. However, it is obvious from the chemical and spectroscopic investigation that two different types of sulfur coexist in two different cage sites in the lazurite structure. The formula $\text{Na}_7\text{Ca}[\text{Al}_6\text{Si}_6\text{O}_{24}]\text{SO}_4(\text{S}_3^-) \cdot \text{H}_2\text{O}$, proposed in the present work, is preferable for lazurite because it accounts for the mandatory presence of a voluminous sulfate group in lazurite structural cages, without which the unit-cell parameter would be as low as in

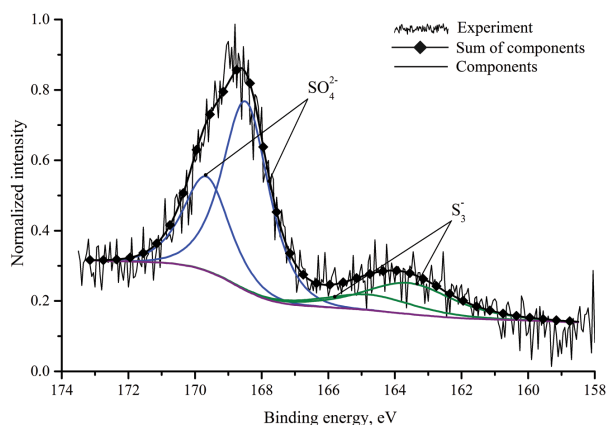


FIGURE 10. S 2p XPS spectra of the dark blue lazurite from the Malo-Bystrinskoe deposit. The peak parameters are given in Table 6.

TABLE 6. XPS data of the S 2p of dark blue lazurite from the Malo-Bystrinskoe deposit

Photoelectron peak	Binding energy (eV)	FWHM (eV) ^a	MPE ^b	MF ^c
S 2p _{3/2}	163.39	3.6	(S ₃) ⁻	0.26
S 2p _{1/2}	164.58	3.6		
S 2p _{3/2}	168.27	2.5	(SO ₄) ²⁻	0.74
S 2p _{1/2}	169.45	2.5		

^a Full-width at half maximum of peak height.

^b Most probable sulfur entities (MPE) from BE values.

^c Mole fraction (MF) calculated from the areas of doublets.

S-sodalite (i.e., <9 Å). It explains the excess of sulfide sulfur atoms as compared to the idealized formula given in the IMA list, and it determines the dark blue “velvet” color of the mineral by the presence of trisulfide radical ion (S_3^-) as a species-defining component.

The important conclusion following from the results of the investigation of S-rich lazurite is the possibility of the incorporation of the radical ion (S_3^-) into the sodalite β -cage of the lazurite structure. This conclusion, drawn on the basis of chemical data and charge-balance requirement, was confirmed by IR, Raman, EPR, and XPS data. This ubiquitous anion is known to be sufficiently stable under elevated T and P parameters and different environmental conditions (Chivers and Elder 2013).

Lazurite, the clathrate-type mineral containing constitutional trisulfide radical anions, may be an effective (S_3^-) sensor due to its stability in isolated cages of the lazurite structure. This may be important because of the predicted high complexation ability of (S_3^-) with heavy and precious metals in hydrothermal solutions (Pokrovski et al. 2015). On the other hand, the matrix isolation phenomenon enabled us to study the behavior of this radical anion over much larger ranges of T and P than would be possible for free species.

Another implication concerns the evaluation of redox conditions of the metasomatic processes. It is highly likely that the $(\text{SO}_4)^{2-}/(\text{S}_3^-)$ ratio depends on oxygen and sulfur dioxide fugacities during lazurite formation (Tauson et al. 2011).

The provenance of lapis lazuli used in antiquity is determined by so-called “strong markers,” mainly based on the type and composition of coexisting minerals in the lazurite-containing rocks (Lo Giudice et al. 2017). A distinctive feature of numerous lazurite samples from deposits in the Baikal Lake area is the presence of specific types of incommensurate structure modulation,

the common one being 41.6 Å, whereas the 61.8 Å modulation described in this paper for high-S lazurite is rare. An additional point is that the types and ratios of cage clusters may be important geochemical markers.

ACKNOWLEDGMENTS AND FUNDING

The authors thank anonymous reviewers and A.G. Bulakh for constructive criticism and useful comments. The research was performed within the framework of state task IX.124.3, registration no. AAAA-A17-117041910035-2. The IR spectroscopy study was partly performed in accordance with state task, registration no. AAAA-A19-119092390076-7. The Raman spectroscopy study was supported by the Russian Foundation for Basic Research, grant no. 18-29-12007. The study of dehydration of samples was carried out with the support of the grant no. RSF 18-72-10085.

REFERENCES CITED

- Arieli, D., Vaughan, D.E.W., and Goldfarb, D. (2004) New synthesis and insight into the structure of blue ultramarine pigments. *Journal of the American Chemical Society*, 126, 5776–5788. <https://doi.org/10.1021/ja0320121>.
- Balassone, G., Bellatreccia, F., Mormone, A., Biagioni, C., Pasero, M., Petti, C., Mondillo, N., and Farnelli, G. (2012) Sodalite-group minerals from the Somma-Vesuvius volcanic complex, Italy: A case study of K-feldspar-rich xenoliths. *Mineralogical Magazine*, 76(1), 191–212.
- Bellatreccia, F., Della Ventura, G., Piccinini, M., Cavallo, A., and Brilli, M. (2009) H₂O and CO₂ in minerals of the hauyne-sodalite group: An FTIR spectroscopy study. *Mineralogical Magazine*, 73, 399–413. <https://doi.org/10.1180/minmag.2009.073.3.399>.
- Bolotina, N.B. (2006) Isotropic lazurite: A cubic single crystal with an incommensurate three-dimensional modulation of the structure. *Crystallography Reports*, 51, 968–976. <https://doi.org/10.1134/S106377450606006X>.
- Chivers, T., and Elder, P.J.W. (2013) Ubiquitous trisulfur radical anion: fundamentals and applications in materials science, electrochemistry, analytical chemistry and geochemistry. *Chemical Society Reviews*, 42, 5996–6005. <https://doi.org/10.1039/c3cs60119f>.
- Clark, R.J.H., and Cobbold, D.G. (1978) Characterization of sulfur radical-ions in solutions of alkylpolysulfides in dimethylformamide and hexamethylphosphoramide and in solid-state in ultramarine blue, green, and red. *Inorganic Chemistry*, 17, 3169–3174. <https://doi.org/10.1021/ic50189a042>.
- Clark, R.J.H., Dines, T.J., and Kurmoo, M. (1983) On the nature of the sulfur chromophores in ultramarine blue, green, violet, and pink and of the selenium chromophore in ultramarine selenium—Characterization of radical-ions by electronic and resonance Raman spectroscopy and the determination of their excited-state geometries. *Inorganic Chemistry*, 22, 2766–2772. <https://doi.org/10.1021/ic00161a024>.
- Climent-Pascual, E., de Paz, J.R., Rodríguez-Carvajal, E., Suard, E., and Sáez-Puche, R. (2009) Synthesis and characterization of the ultramarine-type analog Na₈[Si₆Al₆O₂₄](S²⁻, S³⁻, CO₃)₍₁₋₂₎. *Inorganic Chemistry*, 48, 6526–6533. <https://doi.org/10.1021/ic900438c>.
- Evsyunin, V.G., Sapozhnikov, A.N., Kashaev, A.A., and Rastsvetaeva, R.K. (1997) Crystal structure of triclinic lazurite. *Crystallography Reports*, 42, 938–945. <https://dx.doi.org/10.1134/1.170716>.
- Evsyunin, V.G., Rastsvetaeva, R.K., Sapozhnikov, A.N., and Kashaev, A.A. (1998) Modulated structure of orthorhombic lazurite. *Crystallography Reports*, 43, 999–1002. <http://dx.doi.org/10.1134/1.170884>.
- Fechtelkord, M. (1999) Structural study of Na₈[AlSiO₄]₆(CO₃)₆(HCOO)_{2-2x}(H₂O)_{4x}, 0.2 ≤ x ≤ 1, synthesized in organic solvents: Order and disorder of carbonate and formate anions in sodalite. *Microporous and Mesoporous Materials*, 28, 335–351. [https://doi.org/10.1016/S1387-1811\(98\)00302-3](https://doi.org/10.1016/S1387-1811(98)00302-3).
- Fleet, M.E., Liu, X., Harmer, S.L., and Nesbitt, H.W. (2005) Chemical state of sulfur in natural and synthetic lazurite by S K-edge xanes and X-ray photoelectron spectroscopy. *Canadian Mineralogist*, 43, 1589–1603. <https://doi.org/10.2113/gscanmin.43.5.1589>.
- Gadiyatov, V. (2012) Gems—the stone rainbow of Earth. Voronezh State University, Voronezh (in Russian).
- Gesing, T.M., and Buhl, J.C. (1998) Crystal structure of a carbonate-nosean Na₈[AlSiO₄]₆CO₃. *European Journal of Mineralogy*, 10, 71–77. <https://doi.org/10.1127/ejm/10/1/0071>.
- Gobeltz-Hauteceur, N., Demortier, A., Lede, B., Lelieur, J.P., and Duhayon, C. (2002) Occupancy of the sodalite cages in the blue ultramarine pigments. *Inorganic Chemistry*, 41, 2848–2854. <https://doi.org/10.1021/ic010822c>.
- Hassan, I., and Buseck, P.R. (1989) Incommensurate-modulated structure of nosean, a sodalite-group mineral. *American Mineralogist*, 74, 394–410.
- Hassan, I., and Grundy, H.D. (1984) The crystal structures of sodalite-group minerals. *Acta Crystallographica*, B40, 6–13. <https://doi.org/10.1107/S0108768184001683>.
- (1989) The structure of nosean, ideally Na₈[Al₆Si₆O₂₄]SO₄·H₂O. *Canadian Mineralogist Journal*, 27, 165–172.
- (1991) The crystal structure of basic cancrinite, ideally Na₈[Al₆Si₆O₂₄](OH)₂·3H₂O. *Canadian Mineralogist Journal*, 29, 123–130.
- Hassan, I., Peterson, R.C., and Grundy, H.D. (1985) The structure of lazurite, ideally Na₈Ca₂(Al₆Si₆O₂₄)S₂, a member of the sodalite group. *Acta Crystallographica*, C41, 827–832. <https://doi.org/10.1107/S0108270185005662>.
- Hogarth, D.D., and Griffin, W.L. (1976) New data on lazurite. *Lithos*, 9, 39–54. [https://doi.org/10.1016/0024-4937\(76\)90055-4](https://doi.org/10.1016/0024-4937(76)90055-4).
- Ivanov, V.G., and Sapozhnikov, A.N. (1985) Lazurites of the USSR. Nauka, Novosibirsk (in Russian).
- Li, S., Liu, M., and Sun, L. (2011) Preparation of acid-resisting ultramarine blue by novel two-step silica coating process. *Industrial and Engineering Chemistry Research*, 50, 7326–7331. <https://doi.org/10.1021/ie200343k>.
- Lo Giudice, A., Angelici, D., Re, A., Gariani, G., Borghi, A., Calusi, S., Giuntini, L., Massi, M., Castelli, L., Taccetti, F., and others (2017) Protocol for lapis lazuli provenance determination: Evidence for an Afghan origin of the stones used for ancient carved artefacts kept at the Egyptian Museum of Florence (Italy). *Archaeological and Anthropological Sciences*, 9, 637–651. <https://doi.org/10.1007/s12520-016-0430-0>.
- Ostroumov, M., Fritsch, E., Faulques, E., and Chauvet, O. (2002) Etude spectrométrique de la lazurite du Pamir, Tajikistan. *Canadian Mineralogist Journal*, 40, 885–893. <https://doi.org/10.2113/gscanmin.40.3.885>.
- Pauling, L. (1930) The structures of sodalite and helvite. *Zeitschrift für Kristallographie*, 74, 213–225.
- Pinon, V., Levillain, E., and Lelieur, J. (1992) The S₃ radical as a standard for ESR experiments. *Journal of Magnetic Resonance*, 96, 31–39. [https://doi.org/10.1016/0022-2364\(92\)90285-F](https://doi.org/10.1016/0022-2364(92)90285-F).
- Platonov, A.N., Tarashech, A.N., Belichenko, V.P., and Povarennikh, A.S. (1971) Spectroscopic study of sulfide sulfur in some framework aluminosilicates. Constitution and Properties of Minerals, 5, 61–72 (in Russian).
- Pokrovski, G.S., Kokh, M.A., Guillaume, D., Borisova, A.Y., Gisquet, P., Hazemann, J.-L., Lahera, E., Net, W.D., Proux, O., Testemale, D., and others (2015) Sulfur radical species form gold deposits on Earth. *Proceedings of the National Academy of Sciences*, 112, 13,484–13,489. www.pnas.org/cgi/doi/10.1073/pnas.1506378112.
- Reshetnyak, N.B., Tretyakova, L.I., and Vokhmentsev, A.Y. (1986) Investigation of colour centres in natural lazurite by means of Raman spectroscopy. *Mineralogicheskiy Zhurnal*, 8(5), 49–60 (in Russian).
- Samoilovich, M.I. (1971) An ESR study of sulfur-bearing radical ions in minerals. *Geokhimiya*, 4, 477–483 (in Russian).
- Sapozhnikov, A.N. (1992) Modulated structure of lazurite from deposits in southwestern Pamir. *Soviet Physics, Crystallography*, 37, 470–472.
- Sapozhnikov, A.N., Kaneva, E.V., Cherepanov, D.I., Suvorova, I.F., Ivanova, L.A., and Reznitsky, L.Z. (2012) Vladimirivanovite Na₈Ca₂[Al₆Si₆O₂₄](SO₄, S³⁻, S²⁻, Cl)₂·H₂O, a new mineral of sodalite group. *Geology Ore Deposits*, 54, 557–564. <https://doi.org/10.1134/S1075701512070070>.
- Stuedel, R. (2003) Inorganic polysulfides S_n²⁻ and radical anions S_n^{•-}. In R. Stuedel, Ed., *Elemental sulfur and sulfur-rich compounds II. Topics in Current Chemistry*, vol. 231. Springer.
- Tauson, V.L., Akimov, V.V., Sapozhnikov, A.N., and Kuznetsov, K.E. (1998) Investigation of the stability conditions and structural-chemical transformations of Baikal lazurite. *Geochemistry International*, 36, 717–733.
- Tauson, V.L., Sapozhnikov, A.N., Shinkareva, S.N., and Lustenberg, E.E. (2011) Indicative properties of lazurite as a member of clathrasil mineral family. *Doklady Earth Sciences*, 441, 1732–1737. <https://doi.org/10.1134/S1028334X11120312>.
- Tauson, V.L., Goettlicher, J., Sapozhnikov, A.N., Mangold, S., and Lustenberg, E.E. (2012) Sulfur speciation in lazurite-type minerals (Na₈Ca)₂[Al₆Si₆O₂₄](SO₄, S₂) and their annealing products: A comparative XPS and XAS study. *European Journal of Mineralogy*, 24, 133–152. <https://doi.org/10.1127/0935-1221/2011/0023-2132>.
- Taylor, D. (1967) The sodalite group of minerals. *Contributions to Mineralogy and Petrology*, 16, 172–188.
- Tossell, J.A. (2012) Calculation of the properties of the S₃ radical anion and its complexes with Cu⁺ in aqueous solution. *Geochimica et Cosmochimica Acta*, 95, 79–92.
- Wells, A.F. (1984) *Structural Inorganic Chemistry*. Clarendon Press, Oxford.
- Wong, M.W. (2003) Quantum chemical calculations of sulfur-rich compounds. In R. Stuedel, Ed., *Elemental Sulfur and Sulfur-Rich Compounds II*, 143 p. Springer.

MANUSCRIPT RECEIVED OCTOBER 9, 2019

MANUSCRIPT ACCEPTED JUNE 10, 2020

MANUSCRIPT HANDLED BY KATE KISEEVA